ISBN: 978-3-95450-234-9 ISSN: 2673-5504 doi:10.18429/JACoW-SRF2023-MOPMB078

DESIGN AND PROTOTYPING OF THE ELECTRON ION COLLIDER ELECTRON STORAGE RING SRF CAVITY*

J. Guo†, E. Daly, E. Drachuk, R. Fernandes, J. Henry, J. Matalevich, G. Park, R. A. Rimmer, D. Savransky, JLAB, Newport News, VA, USA
D. Holmes, K. Smith, W. Xu, A. Zaltsman, BNL, Upton, NY, USA

Abstract

Among the numerous RF subsystems in the Electron Ion Collider (EIC), the electron storage ring's (ESR) 591 MHz fundamental RF system is one of the most challenging. Each cavity in the system will handle up to 2.5 A of beam current and supply up to 600 kW beam power under a wide range of voltage. The EIC R&D plan includes the design, fabrication and testing of such a cavity. In this paper, we will report the latest status and findings of the ongoing design and prototyping of this cavity, including the RF and mechanical/thermal design, fabrication design, and the progress of fabrication.

EIC ESR RF SYSTEM REQUIREMENTS

EIC ESR is a high current electron storage ring required to operate at a wide range of beam energy (5-18 GeV) and beam current (0.23-2.5 A average, with one abort gap) [1, 2]. The project plans to build and install 17 SRF elliptical single cell cavities of 591 MHz in the ESR in a single phase before operation starts, providing up to 10 MW beam power for the electron beam. Although the RF/SRF systems for the B factories (such as KEKB/SuperKEKB and PEP-II [3, 4]) have demonstrated this level of beam power in their High Energy Rings (HERs) and the beam current of 2-3 A in their Low Energy Rings (LERs), the EIC ESR will combine both challenges in one ring, imposing more stringent HOM impedance budget per cavity. The wide range of operation voltage, beam current and synchrotron phase requires a factor of 10-20 variation in Qext to minimize the reflected RF power and suppress the Robinson instability of the beam, if all cavities are operating at the same synchrotron phase.

One possibility is to operate some cavities in reversed or defocusing phase (RPO) for low energy cases. This operation mode can increase the single cavity voltage while keeping the vector sum of voltage the same, reducing the required range of Qext variation. Transient beam loading effects induced by the abort gap in the ring can also be mitigated by the higher stored energy in the RPO, in combination with a low R/Q design. This concept has been demonstrated at SuperKEKB [5], although long term operation has not been proven yet. Table 1 shows that with RPO, it's possible to operate the ESR cavities at fixed Qext of ~2×10^5 with tolerable reflected RF power. The RF power values in Table 1 are analytically calculated based on CW beam loading using the peak values.

Simulation by T. Mastoridis with the actual beam time structure and direct feedback showed that the peak forward RF power for the 18 GeV case is about the same as the analytical result; for the 10 GeV case the simulated peak is also similar to the analytical CW value with optimum coupling, and a few percent higher than analytical if we double the Qext; for the 5 GeV 2.5 A all focusing case, the simulated peak is about 10% higher when the Qext is close to optimum, but the peak may increase quickly for higher Qext. With the RPO, the extra RF power needed to compensate the transient is significantly reduced in all cases.

The ESR cavity will have two fundamental power couplers (FPC), each powered by a 200 kW SSA will be installed in the initial phase but will upgrade to 400 kW later to provide the full power. Currently we assume that the cavity will have the capability to operate with full beam power under the all focusing mode, so Qext tuning is required in the full power phase.

The baseline of the cryomodule design contains a single symmetric cavity, with beampipes tapered to 75 mm radius to match the largest available gate valve possible to fit in the space available for the ESR. Two single-cavity cryomodules will be arranged in one straight between two quadrupole magnets. We are also studying the possibility to taper the beampipes to 36 mm radius, making it possible to reuse quadrupole magnets retired from APS, which are also more efficient due to the smaller aperture.

The nominal maximum voltage of each ESR cavity is 4 MV, and the gradient is 15.8 MV/m.

Table 1: Estimate of ESR Cavity Power and Qext for Different Operation Cases, Assuming 17 Cavities in Total

Beam energy (GeV)		18	10	5
Beam current (A, exc gap)		0.272	2.72	2.72
Beam current (A, average)		0.25	2.5	2.5
Beam power/cav (kW, pk)		593	628	218
V total (MV)		61.5	21.7	9.84
All Focusing	Vcav (MV)	3.62	1.28	0.58
	Qext per cav	2.0E5	6E4	2.5E4
	Pfwd/cav, kW	614	680	221
RPO, Focus Cav	Vcav (MV)		3.7	2.0
	Qext		2E5	2E5
	Pfwd/cav (kW)		650	212
RPO, Defocus Cav	Vcav (MV)		3.22	2.0
	Qext		2E5	2E5
	Pfwd/cav, (kW)		629	212
	# of def cav		6	6

Beam power includes synchrotron radiation and HOM losses

* Authored by Jefferson Science Associates, LLC under U.S. DOE Contract No. DE-AC05-06OR23177, with additional support from U.S. DOE Award Number DE-SC-0019287
†jguo@jlab.org

ISBN: 978-3-95450-234-9 ISSN: 2673-5504 doi:10.18429/JACoW-SRF2023-MOPMB078

ESR CAVITY RF AND THERMAL DESIGN

The ESR cavity started with a symmetric design, which was the baseline in the EIC CDR [1]. An asymmetric design was proposed in [6]. After thorough comparison, we adopted the asymmetric design. On one side of the beampipe it has the 137 mm radius to and tapers to 75 mm, and a 75 mm radius beampipe on the other side without tapering. The large beampipe side helps to lower the fundamental mode R/Q as well as to damp HOMs. The pair of FPCs are install on the small beampipe side, providing more room for the FPC warm to cold transition, which is constrained by the transverse size of the cryomodule. Figure 1 shows top view of the model of the cavity string. The major cavity parameters are shown in Table 2.

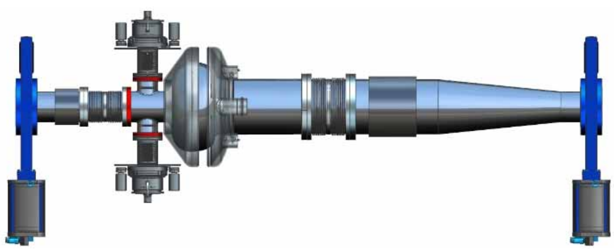

Figure 1: ESR cavity string.

Table 2: Basic Parameters of the ESR Cavity Designs

R/Q (Circ. Def) (Ω)	38
Epk/Eacc	2.01
Bpk/Eacc (mT/(MV/m))	4.87
G (Ω)	307
FPC tip penetration (Qext ~2E5)	9 mm
Approximate total length (gate valve to gate valve)	2.8 m

Qext Tuning and FPC Thermal Analysis

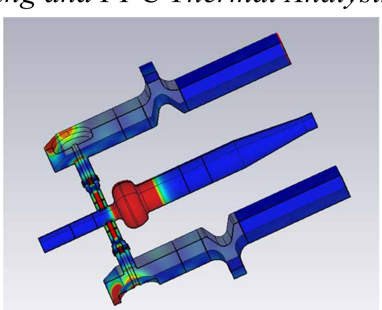

Figure 2. Surface current for the case of 10 GeV 2.71 A all focusing 18 cavities operation, Qext tuned to 6×10^4 (intrinsic Qext=2×10^5).

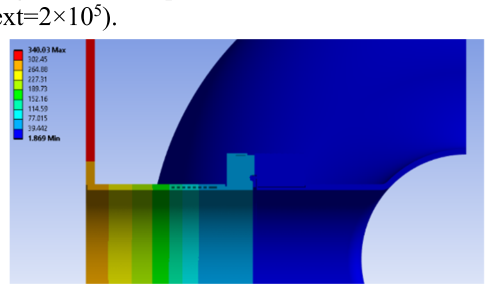

Figure 3. FPC WTC thermal analysis for the case described in Fig. 2.

We choose T stubs to tune the Qext of this cavity. The main concern for this tuner is the strong standing wave between the tuner and the FPC. The analysis in this paper is based on one single matched T [7] on each FPC, as shown in Fig. 2. Such a T's 3rd arm has S_{33}=0, reducing the heating in the stub and making the Qext change more smooth with regard to the movement of the stubs. The intrinsic Qext without tuning is chosen at 2×10^5 now, balanced for the tuning of different operation cases. Simulation shows that we can find one location for the T so that by varying the length of the stub, a Qext range of at least 1×10^4 to 1×10^6 can be achieved with reasonable loss. Other tuner options are also under study [8].

The FPC electric-magnetic field can be simulated with CST frequency domain solver. Beam loading is imitated by a ring on the cavity equator with complex surface impedance. Figure 2 shows the surface current of the case with the voltage and beam loading for 10 GeV 2.71 A operation, Qext tuned from 2×10^5 to 6×10^4, 1.2 MV cavity voltage and 628 kW beam power. This simulated case is about 3 kHz off the optimal detuning, so that the forward RF power is 710 kW (instead of 680 kW for optimal detuning). This detuning can hopefully represent the extra RF power needed to compensate the transient beam loading. The orientation of the doorknob transition and the waveguide was rotated by 90° in this preliminary study, so the simulation size can be reduced with one more symmetry.

CST simulation field data are imported into ANSYS for thermal simulation of the warm-to-cold (WTC) transition. The results for the case above are shown in Fig. 3 and Table 3. The WTC is trace cooled with helium gas. The combination of high FPC power and standing wave produces a high heat load for both 2 K and helium gas. It also generates about 7 kW heat in the doorknob transition and the inner conductor (only ~1 kW was included in this ANSYS simulation). This should be the worst operational case for heat load. For the higher voltage cases (RPO or higher beam energy), the standing wave enhancement will be significantly lower, more than enough to compensate the higher Nb loss; for the lower energy/voltage cases, the beam power will be lower.

Table 3: WTC Thermal Simulation Results for the Case in Fig. 2 with 100 mg/s Helium Flow, Single FPC

Boundary condition	**Heat (W)**	4×11 W heaters
2K	-10.2	
300K	10	45% helix
Air	-7.6	
Water	-1150	
Helium	-70.7	
Temperature (K)		
At extent of Nb	6.5	
Transition Start	45.8	
Transition End	285.7	

ISBN: 978-3-95450-234-9 ISSN: 2673-5504 doi:10.18429/JACoW-SRF2023-MOPMB078

HOM and BLA Analysis

Each ESR cavity will use two beamline absorbers (BLAs) to damp the HOM. The BLA is assumed to be a cylindrical warm SiC absorber SC35 from CoorsTek, using the shrink-fit fabrication technique, similar to the BLAs used in APS-Upgrade but with a larger radius [9, 10]. Currently the ID of the BLAs will be flush with the adjacent beampipes (radius of 75 mm and 137 mm), assuming this minimizes the BLA's impedance and self-heating. The length of the BLAs also need to be minimized due to self-heating.

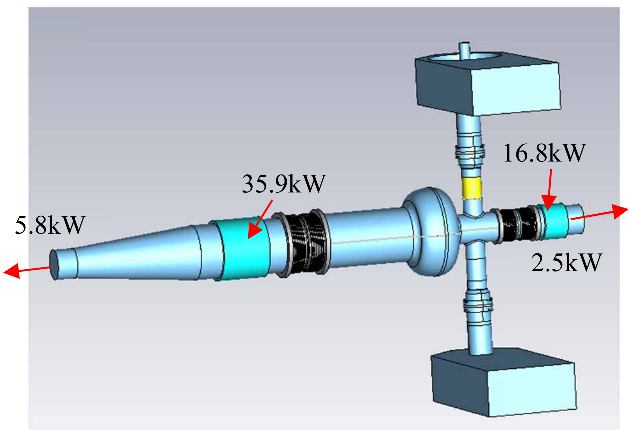

Figure 4: HOM loss power flow, 7 mm 27.6 nC bunches, 2.5 A average current, R 75mm beampipe design.

The monopole and dipole mode impedance of this design was presented in [6] and satisfies the design goal. From the loss factor of CST short range wakefield simulation, monopole HOM power is estimated at 61 kW for 7mm 27.6 nC bunches with 2.5 A beam. This agrees with the loss factor based on the impedance spectrum extrapolated from long range wake simulation, implying that the impedance peaks avoided the major excitation lines.

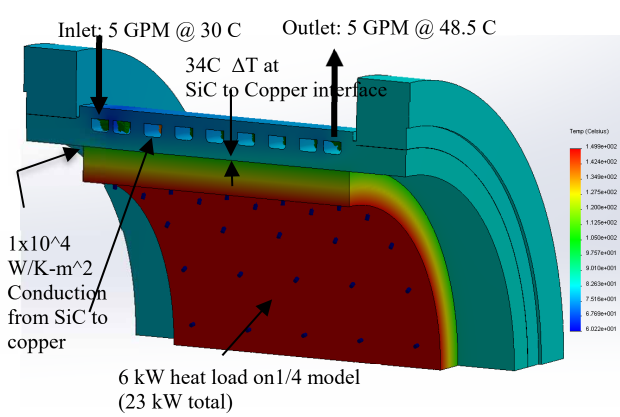

Figure 5: BLA thermal analysis, 7 mm 27.6 nC bunches, 2.5 A average current, R 75 mm beampipe design.

We also made a CST wake simulation monitoring the power flow into the BLAs and beampipes in the cavity, as shown in Fig. 4. With the 7 mm bunch length, assuming all cavities are arranged in the same direction, the large BLA will absorb about 38.4 kW (35.9 kW from this cavity, plus 2.5 kW leaked from the next cavity on the left), while the small BLA will absorb about 22.6 kW. This creates a 0.4 W/cm^2 power density in the R75 mm BLA, which is close to the limit of the thermal design. Figure 5 shows that with known parameters of the absorber material and 22.6 kW HOM power generated at the inner surface, the R75 mm BLA will have ~150°C temperature on the inner surface. Further optimization of this BLA design is ongoing.

The proposed tapering to 36 mm radius beampipes will increase the HOM impedance of the cavity and the total HOM power. However, since the HOM travelling between two cavities will be reduced, the heat in the R75 mm BLA will not increase as much. The study is still underway.

MECHANICAL ANALYSIS

In order to qualify this cavity for operation, a series of ANSYS FEA simulations had to be carried out to parameterize the cavity to ensure it could withstand the stress that will be put on it as well as ensuring that it's mechanical properties would been the ESR requirements.

Table 4: Mechanical Properties of Bare 591 MHz Cavity at 2K

Tuning sensitivity (kHz/mm)	419.25
Stiffness (N/mm)	20683
Tuning force for 600 kHz (N)	29600
Pressure Sensitivity (kHz/torr)	108.2
LFD (Hz/(MV/m)^2)	-4.46

Pressure Analysis

The maximum allowable pressure for this cavity was determined by running FEA pressure stress simulations until the cavity reached its allowable stress point. During this run it was determined that the cavity could withstand over 3.09 Atm of external pressure at room temperature which puts it above the 2.2 Atm relief on the helium circuit shown in Fig. 6.

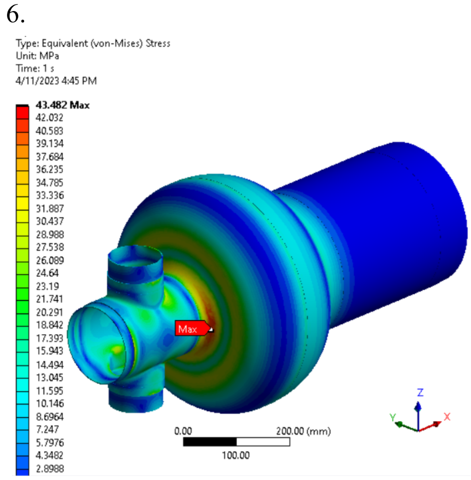

Figure 6: Stress on the cavity with 3 Atm applied external pressure at room temperature [Allowable stress: 43.5 MPa].

ISBN: 978-3-95450-234-9 ISSN: 2673-5504 doi:10.18429/JACoW-SRF2023-MOPMB078

Tuning Analysis

The requirement for this cavity is to be able to be tuned a total of 600 kHz for the worst-case tuning case. The stress FEA was carried out to understand if the cavity would be able to sustain this load without passing the allowable stress. It was determined that with the full tuning load, there would be an almost two-time margin between the tuning stress and the allowable stress as shown in Fig. 7.

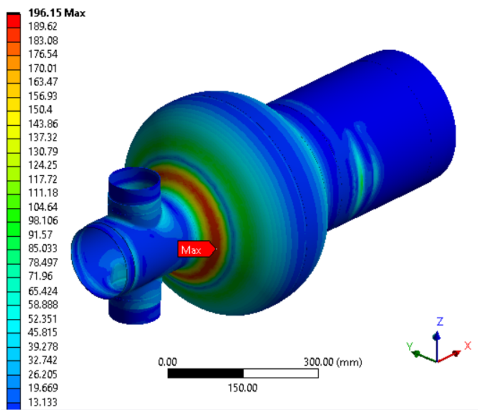

Figure 7: Tuning stress of cavity with 600 kHz applied tuning force at 2 K [Allowable stress: 384.7 Mpa].

PROTOTYPE CAVITY FABRICATION

A functional prototype cavity will be fabricated as part of the R&D effort to understand the fabrication process requirements, analyze the mechanical properties, and verify the RF design of the cavity. All sub-components of the cavity will first be test built from aluminum before being built from niobium. The final milestone of this cavity will be a cryogenic test at 2 K in the Jefferson Lab Vertical Test Area (VTA).

Fabrication Strategy

Whilst this is one of the biggest elliptical cavities ever built at Jefferson Lab, the similarities between this and other built cavities allow for the use of over 30 years of elliptical cavity building experience. In order to fabrication the cavity, it was split up into separate bodies that could be built independently and then EBW or braze together. Fig.8 shows the fabrication breakdown of the cavity. The main parts were the two asymmetric half-cell and then the three sized beampipes. The large beampipe was then also split into three section to allow a full inside/outside EBW on the iris of the large beampipe as well allowing for easy brazing on the other sub-piece.

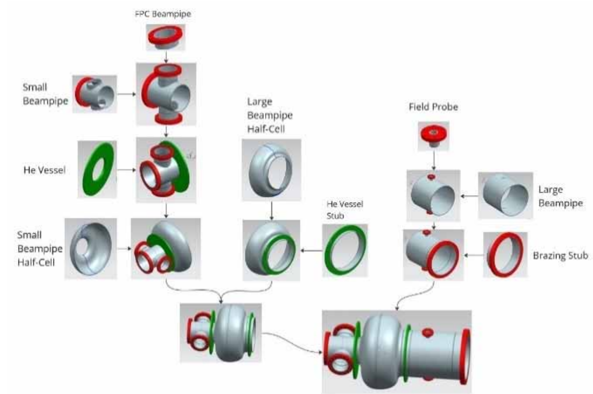

Figure 8: ESR elliptical R&D cavity fabrication plan.

Development of Forming Die

Forming dies for the elliptical cavity half-cells and the beampipe extrusion pulling fixtures were designed with preliminary analysis carried out using LS-DYNA. First, a preliminary model is created to test the basics of the design. This was used to understand the general flow of the material and if damage like crackling and wrinkling would occur. Next, the raw sheet parameters were optimized to eliminate excessive thinning and cracking. During this step, the springback of the formed parts was also analyzed; Fig. 9 shows the simulations for the small beampipe half-cell. This allowed for the construction of springback-compensated dies, where the shape is not built to nominal dimensions, but rather shifted by the predicted springback amount.

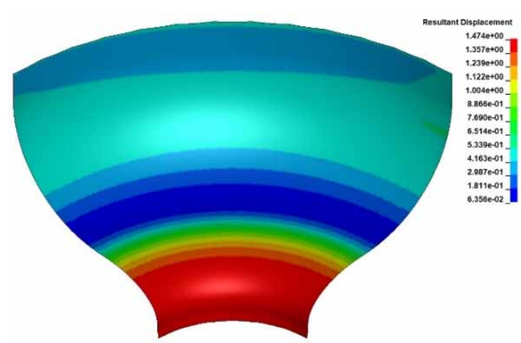

Figure 9: Springback from uncompensated die for Small Beampipe Half-Cell [>1.45 mm of spring back at iris].

Half-cell Aluminum Pressing

A number of forming dies have now been fabricated and have been delivered to Jefferson Lab. Testing has now begun using 6061-O aluminum to verify the validity of the spring back simulation and fix any errors in the dies. Figure 10 shows the pressed part and Fig. 11 shows the topographic data from the pressed part on top of the CAD model. Thus far, only the small beampipe half-cell has been pressed but the springback compensation is looking promising with a max springback of less than 1 mm.

Figure. 10: First half cell pressing with aluminum sheet.

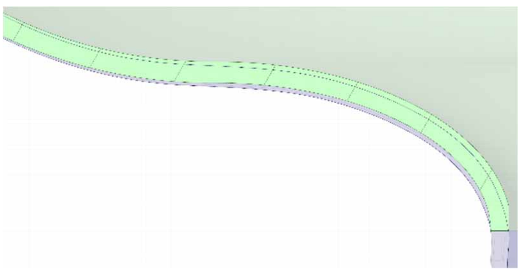

Figure 11: CAD RF shape (green) and aluminum press part (purple).

CONCLUSION AND FUTURE PLANS

We have reported the latest updates of the design and prototyping of the EIC ESR cavity. The bare cavity design is complete and meets the requirements. Prototyping of this bare cavity is ongoing, on schedule for the first vertical testing at the end of this year. The first half cell test press complete with aluminum sheets and will proceed to niobium press soon. The RF/thermal/mechanical design and analysis/optimization of the full cavity string is also moving forward, integrating the Qext tuning network, FPCs, doorknob transitions, BLAs, shielded bellows, RF gaskets, etc.

ACKNOWLEGEMENTS

The authors thank the support from the whole EIC project team. Especially we need to thank G. Grose and V. Pope for their assistance in the prototyping of the cavity.

REFERENCES

[1] F. Willeke *et al.*, "J. Electron Ion Collider Conceptual Design Report 2021", United States, Rep. BNL-221006-2021-FORE, 2021. doi:10.2172/1765663

[2] C. Montag et al., "Electron-Ion Collider Design Status", in *Proc. IPAC'22*, Bangkok, Thailand, Jun. 2022, pp. 1954-1957. doi:10.18429/JACoW-IPAC2022-WEPOPT044

[3] J. Seeman, "Last Year of PEP-II B-Factory Operation", in *Proc. EPAC'08*, Genoa, Italy, Jun. 2008, paper TUXG01, pp. 946-950. https://jacow.org/e08/papers/TUXG01.pdf

[4] Y. Ohnishi, "Recent progress of SuperKEKB project and future prospect", presented at the IPAC'23, Venice, Italy, May 2023, paper TUOGB1, to be published. https://jacow.org/e08/papers/TUXG01.pdf

[5] Y. Morita, "Reverse phase operation", presented at EIC Workshop – Promoting Collaboration on the Electron-Ion Collider, Cockcroft Institute, Oct. 2020, Cockcroft Institute of Accelerator Science and Technology, UK. https://indico.cern.ch/event/949203/.

[6] J. Guo et al., "Design of the Electron Ion Collider Electron Storage Ring SRF Cavity", in *Proc. IPAC'22*, Bangkok, Thailand, Jun. 2022, pp. 1307-1310. doi:10.18429/JACoW-IPAC2022-TUPOTK040

[7] J. Guo, "The Development of the Electrically Controlled High Power RF Switch and Its Application to Active RF Pulse Compression Systems", Ph.D. Thesis, Stanford University, 2008, SLAC-R-919.

[8] W. Xu *et al.*, "Theoretical Model of External Q Tuning for a SRF Cavity with Waveguide Tuner", presented at SRF'23, Grand Rapids, MI, USA, Jun. 2023, paper WEPWB089, this conference

[9] D. Holmes, "R&D toward High Power Warm SiC Beam Line HOM Absorbers", presented at TTC 2020, CERN, Feb. 2020. https://indico.cern.ch/event/817780/.

[10] S. Kim, "HOM Damping in Superconducting Harmonic-Cavity for Advanced Photon Source Upgrade", presented at HOMSC'16, Warnemünde, Germany, 2016. https://indico.cern.ch/event/465683/.